Proceedings of the Seventh International Conference on
Railway Technology: Research, Development and Maintenance
Edited by: J. Pombo
Civil-Comp Conferences, Volume 15, Paper 4.4
Civil-Comp Press, Edinburgh, United Kingdom, 2026
ISSN: 2753-3239, doi: 10.4203/ccc.15.4.4

A Numerical Approach for Predicting Fishplate Stress and Failure at Rail Joints with Unsupported Sleepers

M. Kusuda, T. Tanaka and T. Motono

Track and Structures Department, West Japan Railway Company, Osaka, Japan

Abstract

The unsupported sleeper detection method enables estimation of both the void depth and void length between the underside of an unsupported sleeper and the supporting surface from dynamic track waveforms measured by a track geometry car. As a result, the vertical displacement of the rails during vehicle passage can be readily identified, and this information is increasingly utilized for evaluations such as the fatigue strength of track components. However, at rail joints, decreased accuracy in calculating the void depth is frequently observed, and there are few practical examples of this method's application. Since damage events at rail joints are not fail-safe and managing them is challenging, this study aims to establish a rational approach for preventing fishplate damage. Specifically, we examine the estimation of bending stress generated in fishplates located within unsupported sleeper sections during train passages. In addition, the validity of the present findings is discussed based on a comparison with the actual distribution of unsupported sleepers at rail joints and the number of fishplate failures observed on operational lines.

Keywords: unsupported sleepers, void depth, void length, rail joints, fishplates, axle box acceleration, fatigue life, numerical simulation.

1 Introduction

One of the weak points in railway track structures is the rail joint. Various countermeasures have been implemented for rail joints over the years, with the fundamental approach of eliminating joints through the adoption of continuous welded rail (CWR). However, given Japan's declining population and the resulting future labour shortage, as well as the increasingly challenging business environment for railway operators, it is anticipated that a considerable number of rail joints that cannot be converted to CWR will remain in service. Accordingly, the importance of rail joint management is expected to increase. Damage to joint components, such as fishplates, is not fail-safe and poses a risk to train operation safety. Therefore, careful and prudent management of rail joint components is implemented, and establishing effective damage prevention measures through both physical and organisational reinforcement of rail joint management systems is an urgent task.

In recent years, studies have been conducted to estimate the service life of track components and to establish management standards for components that are significantly affected by train loads—by applying unsupported sleeper detection technologies [1],[2]. For example, research has investigated how unsupported sleepers affect loads acting on the rail fastening system during train operation [3] and has proposed new rail management methods based on the observation that rail bending stresses increase at unsupported sleeper locations [4]. Similarly, it is considered possible to estimate the effects of unsupported sleepers at rail joints, but due to the low estimation accuracy for void depth at these sections, practical application remains difficult.

In response, this study focuses on the fact that, while the precision in estimating void depth is limited, the void length at rail joints can be determined with reasonable accuracy. Based on this, we attempt to estimate the assumed void depth using a mechanical model, and to predict the stress generated in fishplates at rail joints. Using these analysis results, the expected number of fishplate failures was estimated and compared with the actual number of fishplate failures observed in the field to evaluate the validity of the proposed method.

2 Methods

2.1 Calculation method for unsupported sleepers

Unsupported sleepers are determined using the method described in References [1] and [2]. Specifically, as shown in Figure 1, the restored waveform estimated from the dynamic longitudinal level irregularity is applied as the vertical profile of the upper surface of the track-bed along the longitudinal direction of the rail (hereinafter referred to as the "supporting surface"). By calculating the difference between the deflection shape of the track panel and supporting surface (under no train load), it is possible to determine the void depth, which represents the vertical gap between each sleeper and supporting surface.

Although this method has been confirmed to estimate the void depth with high accuracy in locations where the rails are continuous, such as CWR sections, it has been pointed out that the calculation accuracy of the void depth tends to decrease at conventional rail joints where discontinuities are present. Figure 2 shows an example [1].

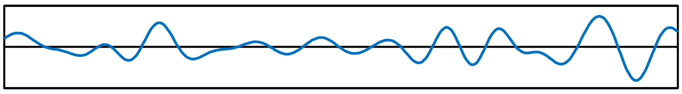

[a] Longitudinal irregularity measured by track geometry vehicle.

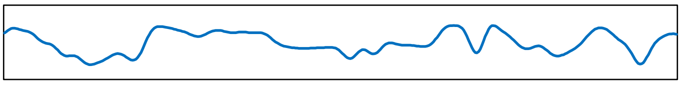

[b] Calculation of longitudinal track shape loaded (restoration waveform).

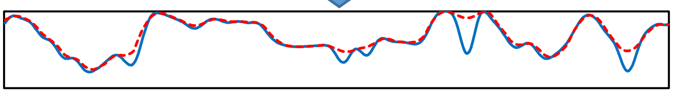

[c] Calculation of deflection by the weight of the track panel installed on the ballast surface which matches the actual longitudinal track shape loaded.
[d] Void represents the distance between the track (red dashed line) and supporting surface (blue solid line) at each sleeper.

Figure 1: Flow of gap calculation of unsupported sleeper [1].

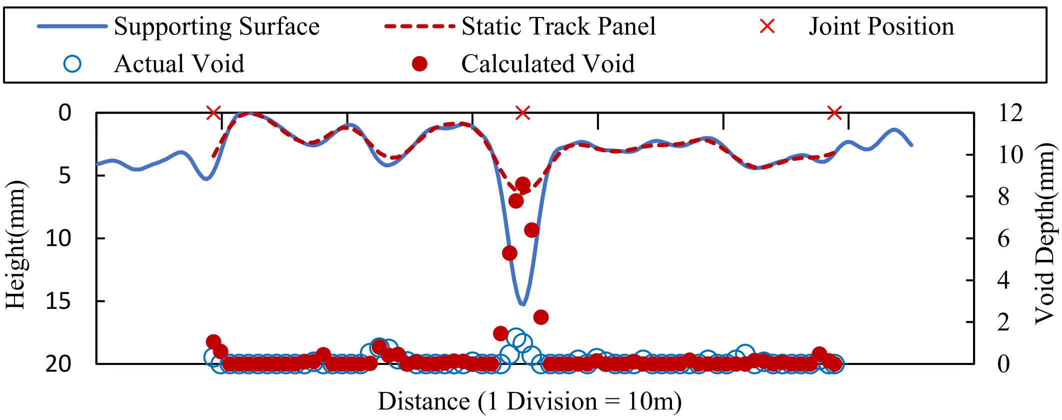

Figure 2: Flow of gap calculation of unsupported sleeper [1].

2.2 Estimation of Unsupported Sleepers at Rail Joints

At rail joints, accurately estimating the void depth is challenging. Therefore, this study attempts to estimate the void depth based on the void length, for which an accuracy sufficient for practical rail management can be obtained. Since the track-bed ballast undergoes elasto-plastic deformation due to repeated train loading, supporting surface is considered to be dependent on the deflection shape of the rail under train loads. Observations of the progression of unsupported sleepers in operational lines (see Figure 3) suggest that the advancement of consecutive unsupported sleepers follows a process of increased void depth, expansion of void length, further increase in void depth, and so on. Based on certain assumptions, supporting surface is calculated numerically to reveal the relationship between void length and void depth.

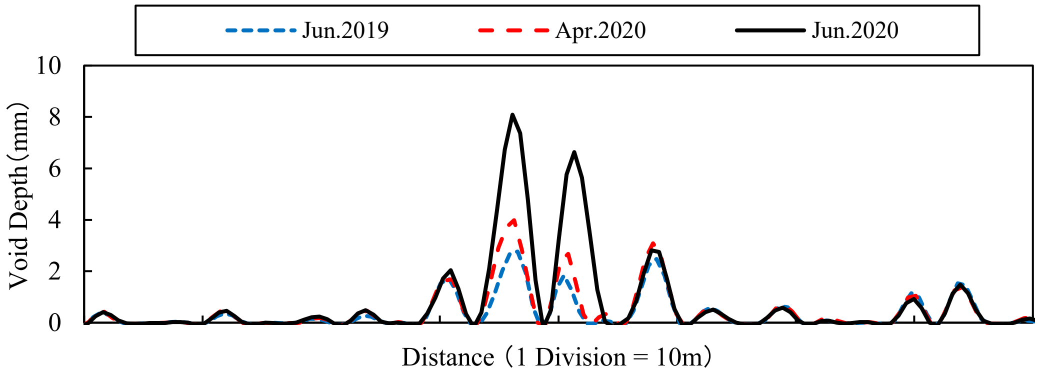

Figure 3: Examples of changes in unsupported sleeper over time.

First, in CWR sections—where the accuracy of void depth estimation is high—this study calculates supporting surface for sections equipped with JIS 50kgN rail and JIS 60kg rail and examines the relation between void length and void depth. These results are compared with those obtained from track inspection data on operational lines. Subsequently, similar analyses are performed for rail joints using JIS 50kgN rails, and the relationship between void length and void depth at rail joints is derived.

In this analysis, the study conditions were determined based on the results of unsupported sleeper analysis for secondary and tertiary grade operational lines, as illustrated in Figure 4. Specifically, the void length was set to 4.55 m or less (corresponding to seven consecutive sleepers at the standard sleeper spacing of 650 mm), which accounts for over 98% of observed cases. The sections analyzed were equipped with JIS 50N rail. In this analysis, the number of unsupported sleeper instances used was 3,322 for CWR sections and 40,932 for jointed rail sections.

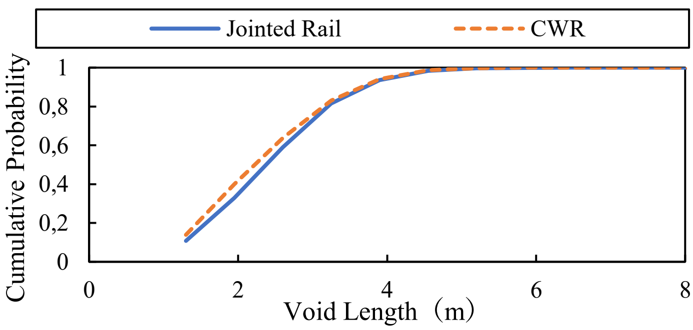

Figure 4: Analysis results of void length observed in operational lines.

For the calculations, a two-dimensional finite element model consisting of beams and nonlinear springs is used, and the following procedure is adopted. The flexural rigidity of the rail near the joints in jointed rail sections was determined using a value converted from the load–deflection relationship obtained in three-point bending tests conducted at the rail joint. Figure 5 shows a schematic of the model used for the calculation of JIS 50N jointed rails.

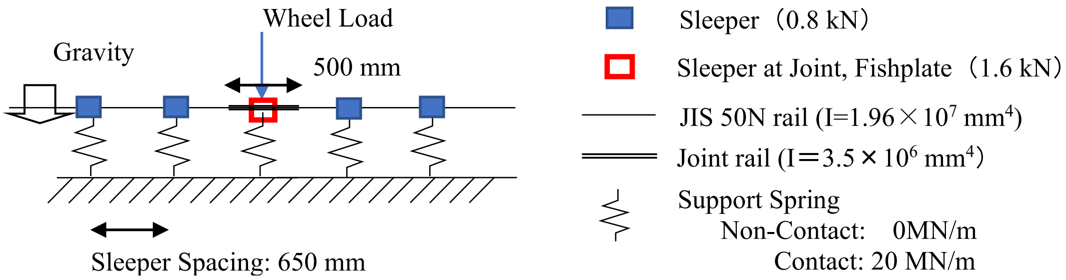

Figure 5: A schematic of the model used for JIS 50N jointed rails.

a) A concentrated load (representing the wheel load) is applied to the rail, and the resulting deformation of the beam is computed. In the case of jointed rails, the load is applied at the rail joint.
b) It is then assumed that the supporting surface conforms to the calculated deformation shape of the beam.
c) The track panel is placed statically on this supporting surface, and the void depth is computed.
d) The concentrated load (wheel load) is applied again at the same loading point, and the deformation of the beam is recalculated.
e) Steps b) through d) are repeated several times to simulate the accumulation of plastic deformation under repeated loads..

2.3 Method for Calculating Fishplate Stress at Unsupported Sleeper Locations

The track panel is statically placed on the supporting surface shape examined in Section 2.2, and the bending moment of the beam directly beneath the loading point is calculated as the concentrated load is gradually increased. The conversion from bending moment to stress is carried out using the relationship between the applied load and the bending stress at the bottom of the fishplate, which was obtained from a three-point bending test performed on a 500 mm-long rail joint.

2.4 Examination of Fishplate Management Methods

To calculate the fatigue life of the fishplate, the fatigue limit for S45C steel—the material used for fishplates—is specified. The fatigue limit is determined based on statistical values obtained from material tests and is calculated on the assumption that the fishplate has reliability equivalent to rails used on conventional lines. Specifically, the fatigue limit is set according to a fracture probability of 0.1% as employed in rail service life calculations for conventional lines [4].

By comparing the stress values calculated in Section 2.3 with the specified fatigue limit, allowable limits for loading under various conditions are established. In this study, the relationship between stress and bending moment is calculated using Equation (1):

$$\sigma = M / (9.6 \times 10^4) \quad (1)$$

where σ is the stress [N/mm^2], M is the bending moment [Nmm]

2.5 Method for Estimating Axle Box Acceleration from Dynamic Wheel Load

Currently, dynamic wheel load measurements are not conducted on a regular basis. Therefore, in establishing management standards, calculations are based on axle box acceleration, which is routinely measured by track geometry cars. The subject vehicle for this analysis is a 51.8 kN commuter-type train, commonly used in practice. There is a strong correlation between wheel load and vertical axle box acceleration. The dynamic wheel load can be expressed as the sum of the static wheel load and the inertial force associated with the unsprung mass, as shown in Equation (2) [5]:

$$P = \kappa_1 P_0 + \kappa_2 W\beta \quad (2)$$

where

P: dynamic wheel load (kN)

P_0: static wheel load (51.8 kN)

κ_1, κ_2: coefficients dependent on track structure ($\kappa_1 = 1.2$, $\kappa_2 = 0.7$)

W: unsprung mass (7.4 kN per wheel)

β: vertical axle box acceleration (G*)   *G: Gravitational Acceleration [=9.8m/s2]

Additionally, when converting axle box acceleration measured at the track geometry car's running speed to the scenario where the subject train is assumed to run at 100 km/h, the velocity impact ratio increment “α” is considered [6]:

$$\alpha = 1.74/ (1 + 0.74V/100) \quad (3)$$

where “V” is the track geometry car's running speed (km/h).

3 Results

3.1 Estimation of Unsupported Sleepers at Rail Joints

The results of the analysis conducted using the method described in Section 2.3 are shown in Figure 6. Focusing first on differences by rail type, the actual void depth for a given void length tends to be greater for JIS 50N rail than for JIS 60 rail. Figure 7 presents analysis results for the observed void length and void depth in sections of operational lines where both rail types are installed. These results similarly show a tendency for void depth to be larger for JIS 50N rail than for JIS 60 rail at the same void length. Although The calculated values display a more pronounced influence of rail stiffness differences, but this method is considered to provide reasonable estimations overall.

Next, regarding differences related to the presence or absence of rail joints, it was found that the void depth at rail joints is approximately 2.3 times greater than that in CWR sections. Figure 8 shows the measured void depth for various void lengths in secondary and tertiary grade track sections on operational lines. In Figure 8, the legend values indicate the void length. Comparing the simulated estimations in Figure 5 with the results in Figure 8, the estimated void depth is somewhat smaller in CWR sections and somewhat larger at rail joints. Possible reasons for this include the dependence of void depth on track maintenance conditions in operational lines, and the possibility that the assumptions regarding plastic deformation in the calculation differed from actual field conditions.

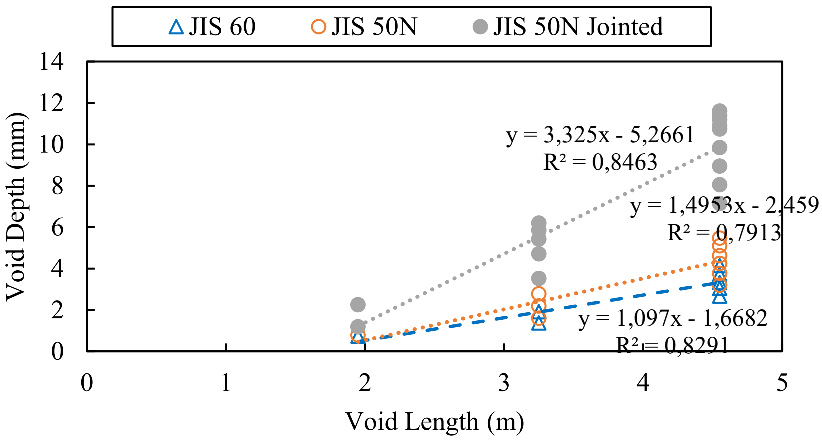

Figure 6: Simulation results of the relationship between void depth and void length for unsupported sleepers.

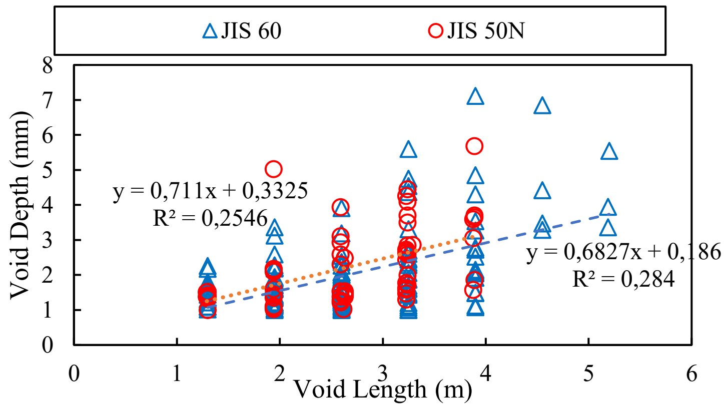

Figure 7: Unsupported sleepers observed in CWR sections of operational lines.

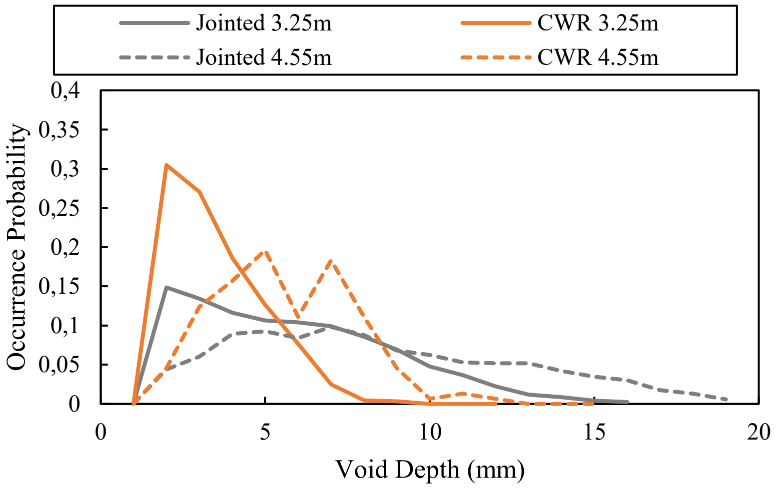

Figure8: Occurrence probability of void depth by void length in operational lines.

3.2 Relationship Among Void, Wheel Load, and Fishplate Stress at Rail Joints

The fishplate stress generated above unsupported sleepers during train operation was estimated using the method described in Section 2.4. The calculation results are shown in Figure 9. In this analysis, the void length conditions were set according to the results shown in Figure 6, and both the maximum and minimum void depth values for each void length were considered. Specifically, for a void length of 1.95 m, void depths of 1.2 mm and 2.3 mm were used; for 3.25 m, 3.5 mm and 6.2 mm; and for 4.55 m, 7.1 mm and 11.6 mm. Data for the same void length are plotted using the same colour.

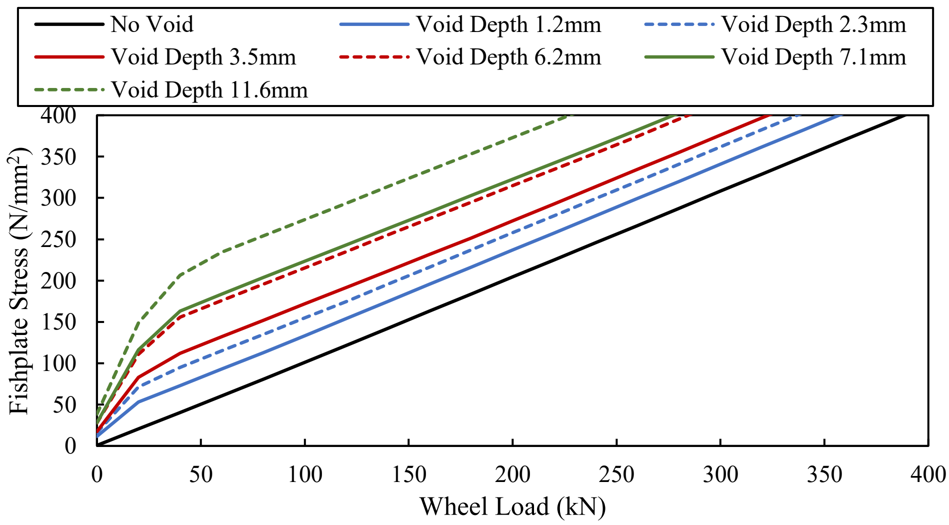

Figure9: Simulation results of fishplate stress generated during train passage over unsupported sleepers.

In the load range above a certain threshold, both wheel load and fishplate stress exhibit a linear relationship, regardless of void length or void depth. The intercept of this linear relationship increases as the void depth increases. Although there are few measurement examples of fishplate bending stress in operational lines, results obtained for bonded insulated fishplates indicate that, at unsupported sleeper locations, fishplate stress under an 80 kN wheel load is approximately 1.5 to 2 times higher. The present estimation results are considered to be in good agreement with those measurements.

3.3 Examination of Fishplate Management Methods

Using the method described in Section 2.4, the stress limit for the fishplate was determined to be 352.9 N/mm². To ensure a conservative assessment, the maximum void depth values for each void length were used (i.e., 2.3 mm for a void length of 1.95 m, 6.2 mm for 3.25 m, and 11.6 mm for 4.55 m). Linear regression was applied in the range above 100 kN wheel load, where the relationship between wheel load and fishplate stress shown in Figure 9 is linear. Based on this regression, the wheel load and axle box acceleration corresponding to the stress limit for each void length were calculated. The results are summarized in Table 1.

Table 1: Maximum Allowable Wheel Load by Void Length.

Void Length	1.95 m	3.25 m	4.55 m
Wheel Load	291.5 kN	237.0 kN	179.8 kN
Axle Box Acceleration	44.3 G	33.8 G	22.7 G

4 Conclusions and Contributions

A numerical calculation method was developed for estimating the stress generated in fishplates located within unsupported sleeper sections. First, the relationship between void length and void depth was calculated, and it was confirmed that the results exhibit trends similar to those observed in operational lines. Based on these findings, the relationship between void length and fishplate stress was determined for rail joints. In load regions above a certain threshold, a linear relationship was observed between wheel load and fishplate stress, indicating that fishplate stress increases with void depth. Furthermore, to prevent fishplate damage, allowable wheel loads and axle box vibration accelerations were proposed for each void length.

The validity of the proposed threshold values was verified as follows. Based on the results in Table 1, linear regression was performed between void length and axle box acceleration. Using the measured void length and speed-corrected axle box acceleration data from the lines described in Figure 8, we determined the number of rail joints where the calculated fishplate stress exceeds the allowable limit. Figure 10 shows the results. Out of 40,932 rail joints where void depth exceeded 1 mm, it was found that 1,481 joints (3.6%) exceeded the stress limit. This indicates that this number of joints could potentially experience damage over several decades of service.

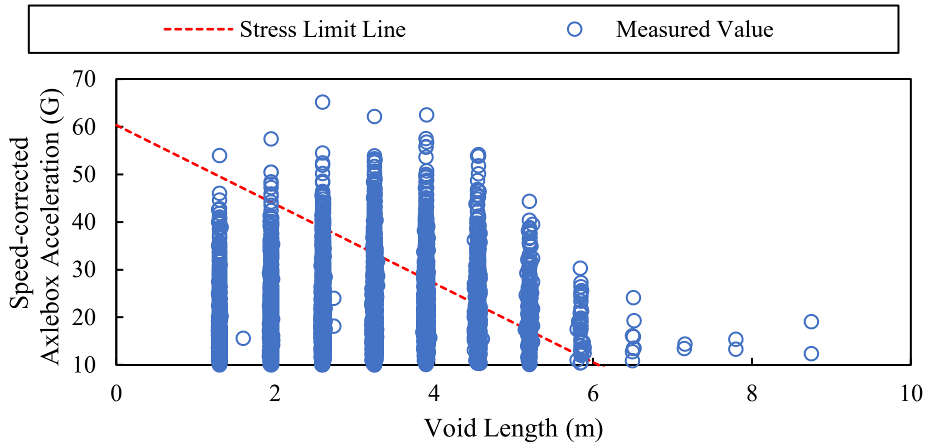

Figure10: Verification Results for the Fishplate Stress Limit.

On the other hand, the actual incidence of fishplate damage (mainly cracking) observed on operational lines is about 0.02% of all installed joints per year. When considering the actual service life, the findings of this study are on the conservative side. One reason for this may be the overestimation of void depth. In addition, this study does not take into account the effects of lateral load or severe environmental conditions such as corrosion, leaving room for improvement in accuracy. Nonetheless, meaningful outcomes regarding management practices to prevent fishplate fractures have been obtained.

Further studies will continue to ensure safe and stable railway operation.

References

[1] M. Kusuda, T. Deshimaru, H. Kataoka," A study on the design method for the ballasted track in consideration of unsupported sleepers", Proceedings of the International Heavy Haul Association STS Conference, 183-191, 2019.

[2] D. Yamanoka, M. Kusuda, H. Tanaka, M. Matsumoto, H. Kataoka, " Proposal for Unsupported Sleeper Detection Method and Utilization in Track Maintenance", QR of RTRI, Vol.63, No.1, 2022.

[3] T. Deshimaru, H. Kataoka, Y. Sonoda: Effect of Track Supporting Condition on Distributed Force Acting on Rail Fastening System, Journal of Railway Engineering, JSCE (in Japanese), No.23, pp.317-324, 2019.

[4] M. Hosoda, N. Takahashi, T. Deshimaru: Fatigue life evaluation of aged rails focusing on the state of hanging sleepers and rail-head surface irregularities that affect rail stress, Transactions of the JSME (in Japanese), Vol.91, No.941, 2025.

[5] Y.Sunaga, I.Sano, T.Ide, "A Method to Control the Short Wave Track Irregularities Utilizing Axlebox Acceleration", QR of RTRI, Vol.38, No.4, 1997.

[6] Railway Technical Research Institute ed., Design Standards for Railway Structures and Commentary (Track Structure) (2011), pp.228-231 (in Japanese).